

Real-coded lattice gas model for ternary amphiphilic fluids

Tomonori Sakai*

Centre for Computational Science, Queen Mary College, University of London, Mile End Road, London E1 4NS, United Kingdom

Yu Chen[†] and Hirotsada Ohashi[‡]

Department of Quantum Engineering and Systems Science, University of Tokyo, 7-3-1 Hongo, Bunkyo-ku, Tokyo 113-8656, Japan

(Received 27 September 2001; published 19 February 2002)

We have developed an amphiphilic surfactant model in the framework of the *real-coded lattice gas* (RLG), in order to analyze the dynamics and structure of ternary fluids. Formation of both the oil-in-water and the bicontinuous microemulsion phases, as well as the reduction of surface tension by adsorption of surfactant at interface are successfully reproduced in numerical simulations. Our model is simple in terms of description and implementation, however, complex structures and dynamic behavior of the ternary fluids emerge from the collective dynamics of the RLG and surfactant particles.

DOI: 10.1103/PhysRevE.65.031503

PACS number(s): 83.80.Qr, 05.10.-a, 82.70.Uv

I. INTRODUCTION

Surfactants could reduce the interfacial tension and thus have been utilized as detergents in our daily lives and industrial fields. Typically, a surfactant molecule has a nontrivial structure, consisting of a hydrophilic head and a hydrophobic tail. This molecular structure leads to the formation of various kinds of structures in solvents, and the emulsification in ternary fluids composed of water, oil, and surfactants. The formation of these structures is due to the energetic preference for the surfactant to adsorb to interfaces, with concomitant reduction of surface tension. These unusual properties make the research of surfactant systems one of the most interesting and exciting topics.

Fluids containing surfactant molecules often exhibit complicated structures and dynamics at both the macroscopic and the microscopic scales. Additionally, they often exhibit complex dynamical phenomena. Numerical analyses by solving Navier-Stokes equations, the continuous and averaged description of fluids, become inappropriate due to the breakdown of the underlying continuous and uniform assumptions. Microscopic fluid models are good candidates for the simulation of surfactant systems, due to that molecular structures can be explicitly taken into account in a very natural and rather easy way.

A number of reports on the simulation of surfactant systems by microscopic approaches have been published, either using the molecular dynamics (MD) [1] or the Monte Carlo [2] methods. These methods provide realistic simulations, but they are far from practical in terms of their computational costs. Simulations using the simplified MD, which allow us to do the calculations with reasonable costs, have thus also been tried, e.g., lattice gas automata (LGA) [3–5] and lattice Boltzmann method (LB) [6]. Our approach here is to model the behavior of surfactant molecules in a bottom-up

way, as is done in LGA, rather than in a top-down way, as in the free energy LB approach. In LGA, one can reduce the degree of freedom of particles by using discrete space and time, and make particles undergo collisions as momentum-conserving state changes. Boghosian and co-workers [3] succeeded in modeling surfactant systems in the framework of the two-phase version of LGA. They also indicated the applicability of their model to nonequilibrium phenomena, which had never been accomplished by other methods. Their work was further developed to model three-dimensional (3D) amphiphilic fluids [4] and flow through porous media [5]. However, LGA are known to suffer great difficulties in accurately reproducing the physics of real fluids and in naturally dealing with the energy transport. In addition, the restriction of discrete lattices lead to the rather complicated collision rules, especially in 3D geometries. On the other hand, the real-coded lattice gas (RLG) to which we implement the surfactant model is a strong method in respect of solving these problems of LGA.

In the following text, we first briefly introduce the RLG and the real-coded immiscible lattice gas RILG, which is the extended version of RLG for binary fluids. Then we will describe the surfactant model and its implementation to the RILG. Finally we show numerical results reflecting some essential features of surfactants in ternary fluids.

II. RLG AND RILG

The RLG evolves by a particle propagation process and a multiparticle collision process. Each particle updates its location in the propagation process by $\mathbf{r}' = \mathbf{r} + \mathbf{v}$, and its velocity in the collision process by $\mathbf{v}' = \mathbf{V} + \sigma(\mathbf{v} - \mathbf{V})$, where \mathbf{V} is the mean velocity of the center of mass in the collision cell and σ is a rotation operator. In these equations primes denote values after collisions. Mass, momentum, and energy are locally conserved during the collision process. Velocity distributions of particles will be that of the Maxwell-Boltzmann when the system is relaxed to an equilibrium state. The coarse-grained macroscopic behavior of the RLG has been proved to follow the solution of the Navier-Stokes equations [7].

*FAX: +44-(0)20-7882-7794.

Email address: T.Sakai@qmw.ac.uk

[†]FAX: +81-3-5800-6857. Email address: chen@q.t.u-tokyo.ac.jp[‡]Email address: ohashi@q.t.u-tokyo.ac.jp

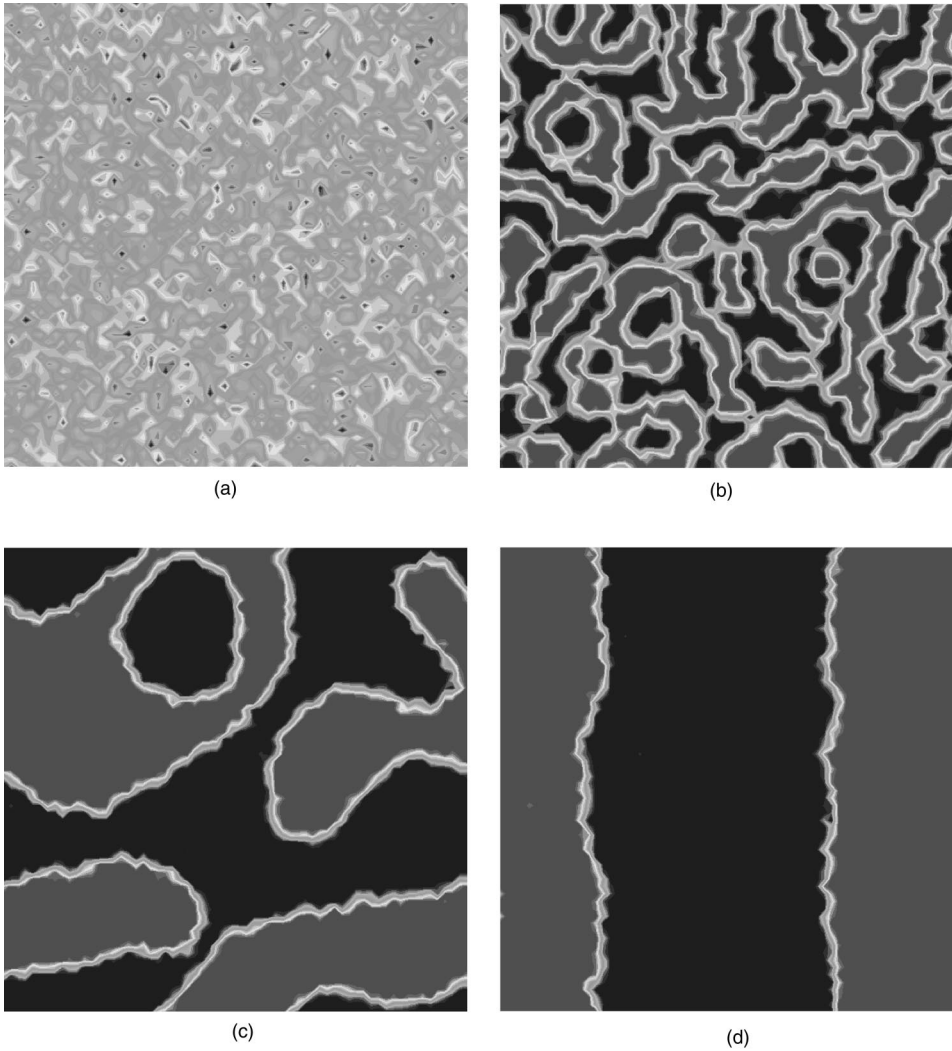


FIG. 1. Two-phase separation in RILG simulation. Randomly distributed particles of two different colors in the initial state segregate each other, until two macroscopic domains are formed. Parameters are the following: system size 64×64 , number density 10, temperature of the system 0.2.

The RLG model for the single-phase thermohydrodynamics introduced above, has been extended into a model for the immiscible binary fluids (we call this model the RILG [8]) by introducing two colors, *red* and *blue*, given by the color charge C_n of the n th particle,

$$C_n = \begin{cases} +1 & \text{if it is a red particle,} \\ -1 & \text{if it is a blue particle.} \end{cases} \quad (1)$$

Similar to the Rothman-Keller's two-phase LGA model [9], an attractive force between particles of the same color and a repulsive force between particles of different colors is applied by defining the color flux vector

$$\mathbf{Q}(\mathbf{r}) = \sum_n^{N(\mathbf{r})} C_n [\mathbf{v}_n - \mathbf{V}(\mathbf{r})], \quad (2)$$

and the color field vector

$$\mathbf{F}(\mathbf{r}) = \sum_i w_i \frac{\mathbf{R}_i}{|\mathbf{R}_i|} \sum_n^{N(\mathbf{r}_i)} C_n, \quad (3)$$

where $N(\mathbf{r})$ is the number of particles in the local cell, \mathbf{v}_n the velocity of the n th particle, $\mathbf{V}(\mathbf{r})$ the mean velocity of particles in a cell. The weighting factors are defined as $w_i = 1/|\mathbf{R}_i|$, where $\mathbf{R}_i = \mathbf{r} - \mathbf{r}_i$, where \mathbf{r}_i is the location of the center of i th neighboring cell. The range of counter i differs according to the definition of the neighbors. With 2D Moore neighbors, for example, i would count from 0 to 7. One can model the phase dynamics of an immiscible binary fluid by choosing a rotation angle for each collision process such that the color flux vector points in the same direction as the color field vector after the collision.

Figure 1 shows the simulation of binary phase separation using this model. Surface tension between the two fluids is verified to obey the Laplace's law, see Fig. 2. Also, the domain growth in the phase separation process are characterized with two distinct rates (see Fig. 3), namely, a slow growth rate $R \sim t^{1/2}$ in the initial stage and a fast growth rate $R \sim t^{2/3}$ later, as has also been observed in other studies [10]. (In this respect, thorough investigations considering the size effects [11], which have not been done in this study, will produce interesting results from which more systematic conclusions may be drawn.)

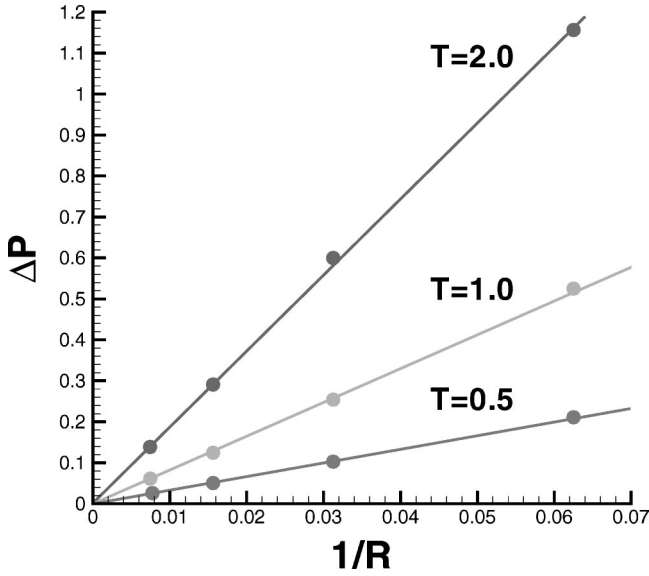


FIG. 2. Verification of Laplace’s law for RILG. The pressure difference between the inside and the outside of a droplet of radius R , $\Delta P = P_{in} - P_{out}$, was measured in a system of the size $4R \times 4R$ ($R = 16/32/64/128$), averaged over 10 000 time steps. The error bars are smaller than the symbols. T is the “temperature” which can be regarded as the indicator of averaged kinetic energy of particles and is defined by $T = kT^*/m$ (k is the Boltzmann constant, T^* is the absolute temperature, and m is the mass of the particle).

III. THE SURFACTANT MODEL

A typical surfactant molecule has a hydrophilic head and a hydrophobic tail. We model this structure by introducing a different type of particle. Figure 4 is a schematic description of the two-dimensional particle model. A and B correspond

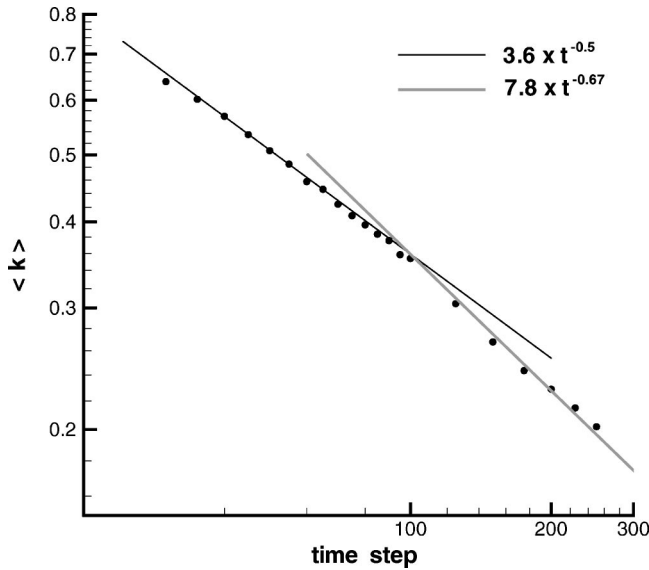


FIG. 3. Temporal evolution of the characteristic wave number in RILG simulations of binary phase separation, averaged over seven independent runs. The domain growth is characterized by two distinct rates, namely, a slow growth rate $R \sim t^{1/2}$ in the initial stage and a fast growth rate $R \sim t^{2/3}$ later.

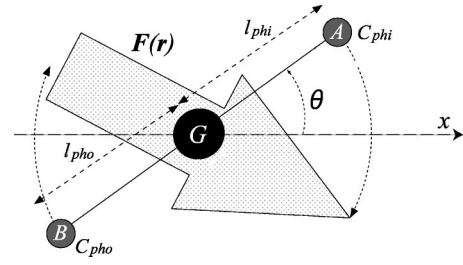


FIG. 4. The schematic description of the 2D surfactant model.

to the hydrophilic head and the hydrophobic tail. G is the center of mass of the surfactant particle. Color charges C_{phi} and C_{phi_o} are installed in A and B , respectively. If we take the background RLG particles as water particles whose color charges are positive, C_{phi} and C_{phi_o} should be set as $C_{phi} > 0$ and $C_{phi_o} < 0$. The attractive interaction between A and water particles and the repulsive interaction between A and oil particles (about B , vice versa) are described. For simplicity, the mass of the surfactant particle is assumed to be concentrated at G , the center of mass. We previously modeled a surfactant by introducing structured particles whose masses are distributed as a dumbbell and succeeded in simulating micelle formation in an aqueous environment [12]. However, the current model provides us with greater simplicity especially in describing the rotational motions of surfactant particles, though (as would be shown later) the ability to reproduce those essential properties of surfactant solutions is adequately retained.

To summarize the model, it has a nontrivial color dynamics, whilst the momentum exchange with its neighboring particles is the same as that of usual RLG point particles. There is thus no need to explicitly consider the effect of rotational motions of the surfactant particle, which reduces the degree of freedom of surfactant particles to only three parameters, that is, the location, the orientation angle, and the translation velocity.

Calculations of the color flux $F(r)$ and the color field $Q(r)$ resemble those in the RILG. For the calculation of $F(r)$, we use Eq. (2), without taking the contributions of surfactant particles into account. Note that motions of A and B only result in suppressing the tendency of $F(r)$ and $Q(r)$ to overlap each other, because they would not influence the “noncolor” momentum exchanges. $Q(r)$ will be determined by considering both the distribution and the structure of surfactant particles. When a surfactant particle is located at r_G with an orientation angle θ (see Fig. 4), A and B ends of the particle are located at

$$\mathbf{r}_A = \begin{pmatrix} r_{Ax} \\ r_{Ay} \end{pmatrix} = \begin{pmatrix} r_{Gx} \\ r_{Gy} \end{pmatrix} + \begin{pmatrix} \cos \theta \\ \sin \theta \end{pmatrix} l_{phi}, \quad (4)$$

$$\mathbf{r}_B = \begin{pmatrix} r_{Bx} \\ r_{By} \end{pmatrix} = \begin{pmatrix} r_{Gx} \\ r_{Gy} \end{pmatrix} - \begin{pmatrix} \cos \theta \\ \sin \theta \end{pmatrix} l_{phi_o}. \quad (5)$$

In these equations l_{phi} and l_{phi_o} are the distance between G and the hydrophilic end (A in Fig. 4), and the distance between G and the hydrophobic end (B in Fig. 4). We then add

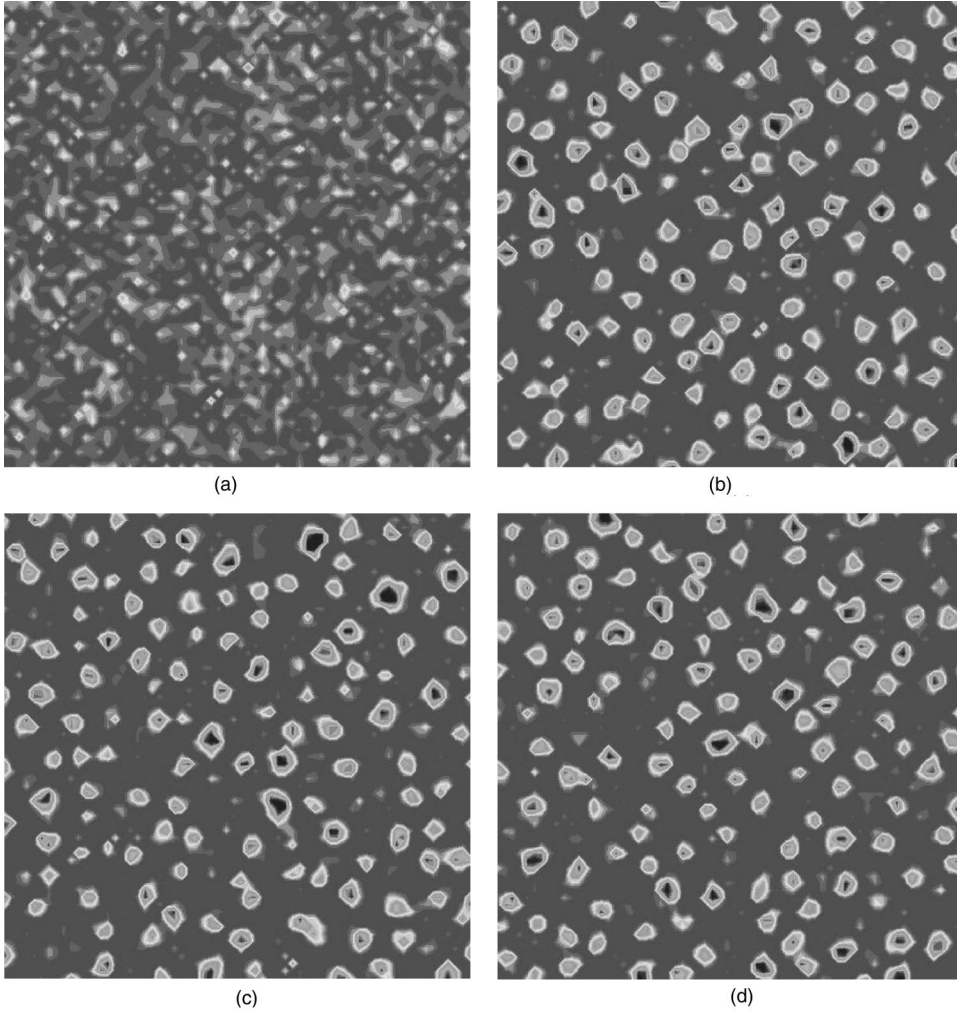


FIG. 5. A ternary RLG simulation of oil-in-water microemulsion. Parameters are the following: system size 64×64 , number density of RLG particles 10, the ratio of water:oil:surfactant 9:1:1, temperature of the system 0.2, color charges for hydrophilic and hydrophobic ends $C_{phi} = 10.0$, $C_{pho} = -10.0$.

the color charge C_{phi} and C_{pho} to cells locating at \mathbf{r}_A and \mathbf{r}_B , which corresponds to modifying Eq. (1) into

$$C_n = \begin{cases} +1 & \text{if it is a red RLG particle,} \\ -1 & \text{if it is a blue RLG particle,} \\ C_{phi} & \text{if it is a hydrophilic head,} \\ C_{pho} & \text{if it is a hydrophobic tail.} \end{cases} \quad (6)$$

Equation (3) will be used as it is.

After calculating the color flux and the color field in each cell, we choose a rotation angle using the same method of RILG, namely, the color flux vector overlaps the color field vector.

Finally, the orientation angle θ of each surfactant particle, after the momentum exchange, is set in a way that it overlaps with the color field, which can be expressed as

$$\begin{pmatrix} \cos \theta \\ \sin \theta \end{pmatrix} = \frac{\mathbf{F}(\mathbf{r})}{|\mathbf{F}(\mathbf{r})|}. \quad (7)$$

IV. SIMULATIONS AND DISCUSSION

Immiscible binary fluids reach their equilibrium states when the whole system becomes completely separated into

two distinct domains. As previously demonstrated, the phenomenon is correctly reproduced in the RILG simulations. With the addition of the surfactant, the binary phase separation can be arrested and the microemulsion phase will be formed. Two kinds of microemulsion phases can be formed depending on the relative amount of the oil/water/surfactant. One possibility is the “oil-in-water” phase where fine oil droplets stay suspended in the bulk water region with their surface surrounded by the surfactant (the “water-in-oil” phase v.v.). When the relative amount of water and oil are nearly equal and sufficient surfactant is present, bicontinuous phase is formed where surfactant, water and oil are bicontinuous in complex tubular shapes.

Figure 5 shows the phase dynamics of the ternary fluid where the ratio of water, oil, and surfactant is 9:1:1. We can observe that after a very short time the system reaches an equilibrium state where small oil droplets are dispersed in the whole system. It is very different from the monotonous progression of the phase separation in the immiscible binary fluids. Our surfactant model works in the same way as real surfactants, that is, bringing about dispersion and suspension effects in ternary fluids. In this model, water/oil and hydrophilic heads/hydrophobic tails are symmetrically treated, so that “oil-in-water” phases and “water-in-oil” phases are completely equivalent.

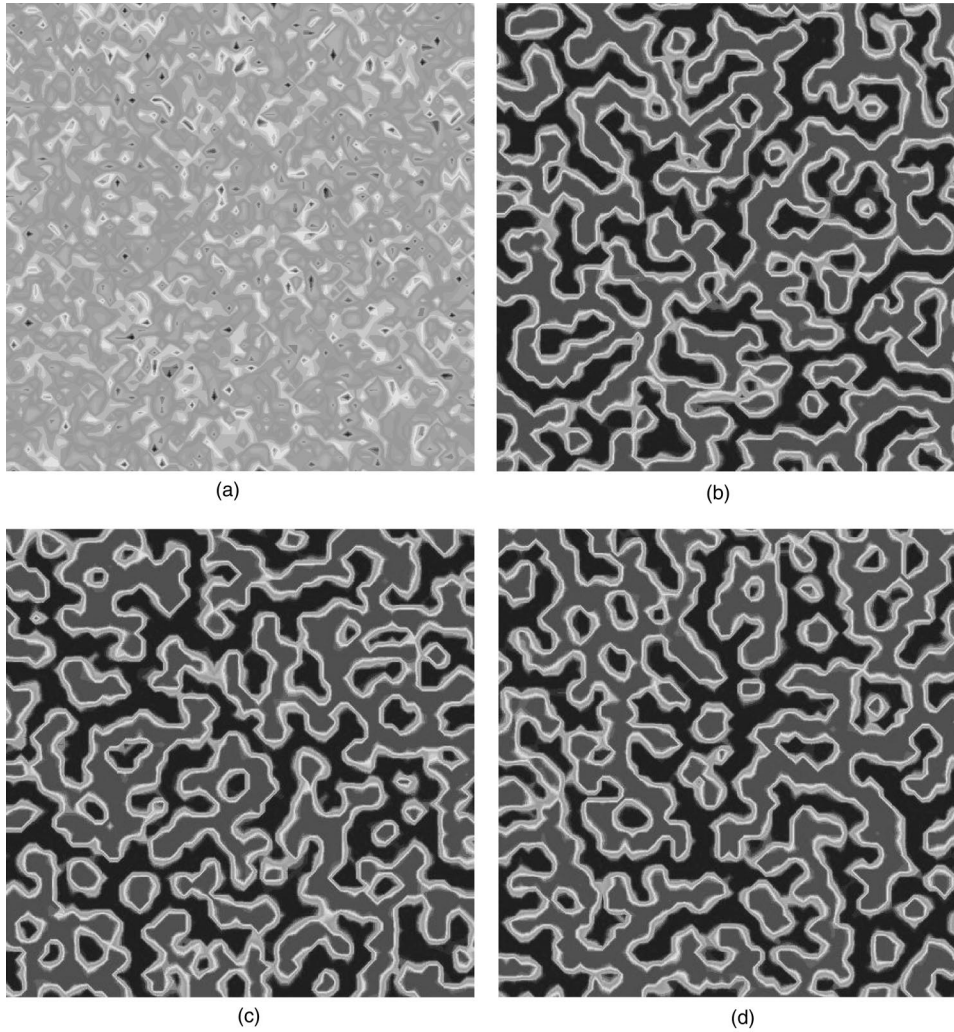


FIG. 6. A ternary RLG simulation of the formation of the bicontinuous phase. Parameters are the following: system size 64×64 , number density of RLG particles 10, the ratio of water/oil/surfactant 1:1:1, temperature of the system 0.2, color charges for hydrophilic and hydrophobic ends $C_{phi} = 10.0$, $C_{pho} = -10.0$.

Figure 6 shows the phase dynamics when we increased the relative amount of oil and surfactant so that the relative ratio to water became 1:1:1. Again we did not observe the monotonous progression of the phase separation, but formation of the bicontinuous phase was observed at a very early stage essentially without any further change.

These visual observations can be quantified by calculating the circularly averaged structure factor $S(k, t)$. Some snapshots in the temporal evolution of $S(k, t)$ are plotted in Fig. 7. The figure also shows the results of the binary phase separation for comparison. In the latter case, a clear peak in the distribution of the wave number emerges after a short time progression. Thereafter the peak increases its height while shifting towards a smaller wave number until the system fell into an equilibrium state. By contrast, in the formation of bicontinuous phase the structure factor has a much broader peak by comparison with the very sharp peaks present in binary phase separation. This fact indicates the formation of complex structures with multiple characteristic length scales in the bicontinuous phase.

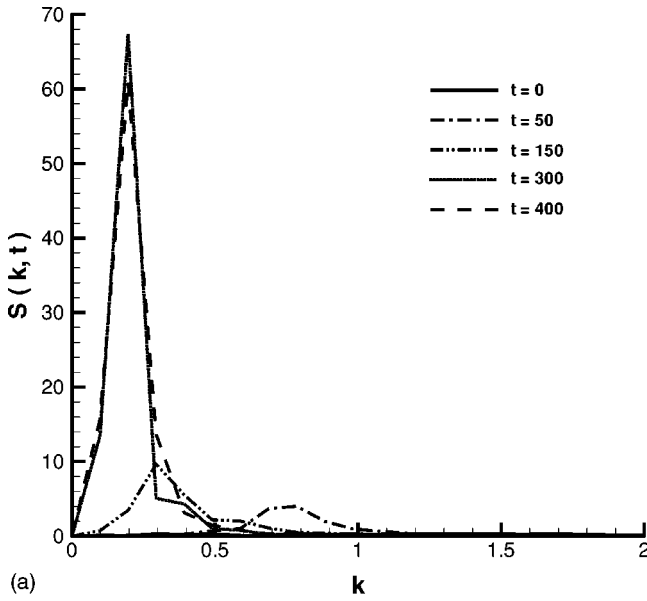
Using these results we calculated the characteristic wave numbers by $\langle k \rangle = \int |k| S(k, t) / \int S(k, t)$, the inverse of which is a measure of the average domain size. The results are plotted in Fig. 8 where the upper solid line denotes the evo-

lution in the bicontinuous phase and the lower dashed line denotes that in the binary separated phase. We clearly observe that the domainal growth is suppressed by adding the surfactants.

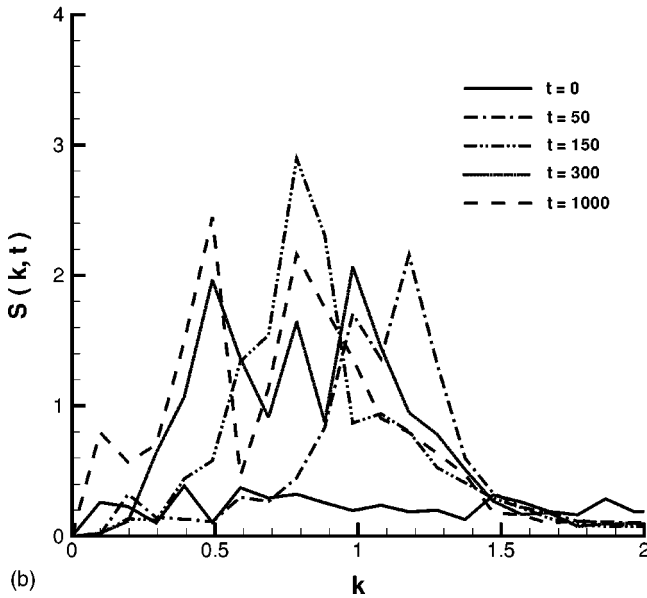
We also investigated the effect of surfactants on the surface tension. In the analysis we used the mechanical definition of the surface tension for a flat interface perpendicular to y axis, that is,

$$\sigma = \int_{-\infty}^{\infty} [P_N(y) - P_T(y)] dy, \quad (8)$$

where $P_N(y)$ and $P_T(y)$ are the pressures in the normal and tangential directions to the interface, respectively. The test system is 32×128 with a flat oil-water interface initially formed at $y = 64$. When there is no surfactant in the system the operation of rotating color flux relative to the color field causes a significant drop of $P_T(y)$ in the vicinity of the interface, while $P_N(y)$ remains almost constant throughout the system. As the amount of added surfactant increases, the color field will no longer be aligned with the normal direction of the interface so that the peak drop in $P_T(y)$ declines and finally vanishes when there is sufficient amount to form the bicontinuous phase, see Fig. 9. In the bicontinuous phase



(a)



(b)

FIG. 7. Temporal evolutions of the structure factor. In the formation of the bicontinuous phase (right) the structure factor has a much broader peak by comparison with the very sharp peaks present in the binary phase separation (left).

the whole system is completely isotropic and thus the surface tension obtained by Eq. (8) becomes nearly zero, making it meaningless to continue the measurement with further increased amount of surfactant. However, as long as the initial flat interface is maintained (as shown in Fig. 10), the measurement of the surface tension is meaningful by taking an average over sufficiently long time steps. Figure 11 shows that the surface tension decreases as the concentration of the surfactant increases and that the larger the absolute values of color charges C_{pho} and C_{phi} is the faster the surface tension decreases. These results, therefore, indicate the effectiveness of our surfactant model in lowering the surface tension and the close connection between the microscopic model parameters and the macroscopic surfactant phase behavior.

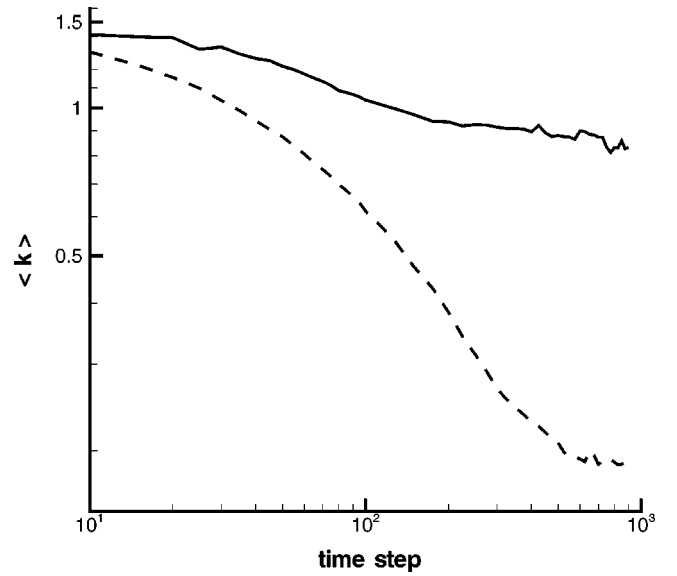


FIG. 8. Comparison of the temporal evolution of the characteristic wave numbers in the formation of the bicontinuous phase (solid line) and the binary phase separation (dashed line). The data were averaged over seven independent runs in the binary case, and three in the ternary case.

V. CONCLUSIONS

We have modeled surfactant molecules by particles of usual mass profiles but with special structures and implemented the model in RILG.

In a series of numerical simulations using our ternary model, we observed that due to the presence of the surfactant binary phase separation is arrested, resulting in the formation of a stable microemulsion phase. The surface tension is low-

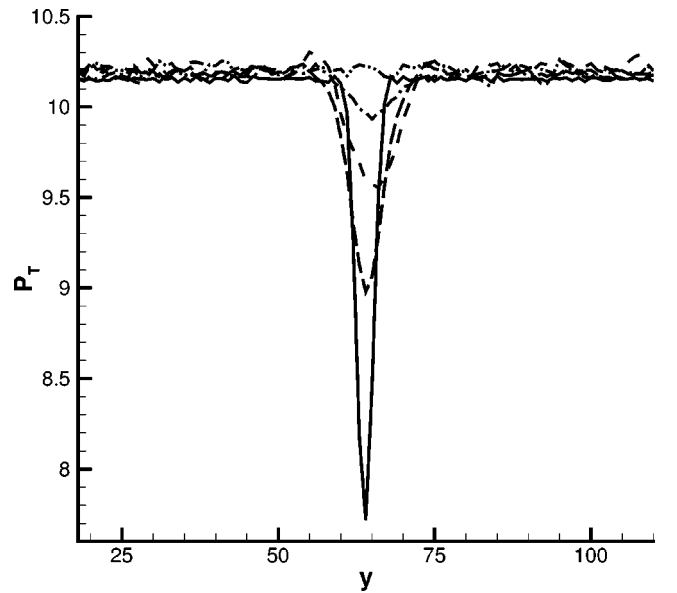


FIG. 9. Distribution of P_T for varying concentrations of the added surfactant, averaged over 10 000 time steps. From the lowermost, the surfactant concentrations are 0%, 5%, 25%, 37.5%, and 50%. Color charges for hydrophilic and hydrophobic ends $C_{phi} = 1.0$, $C_{pho} = -1.0$.

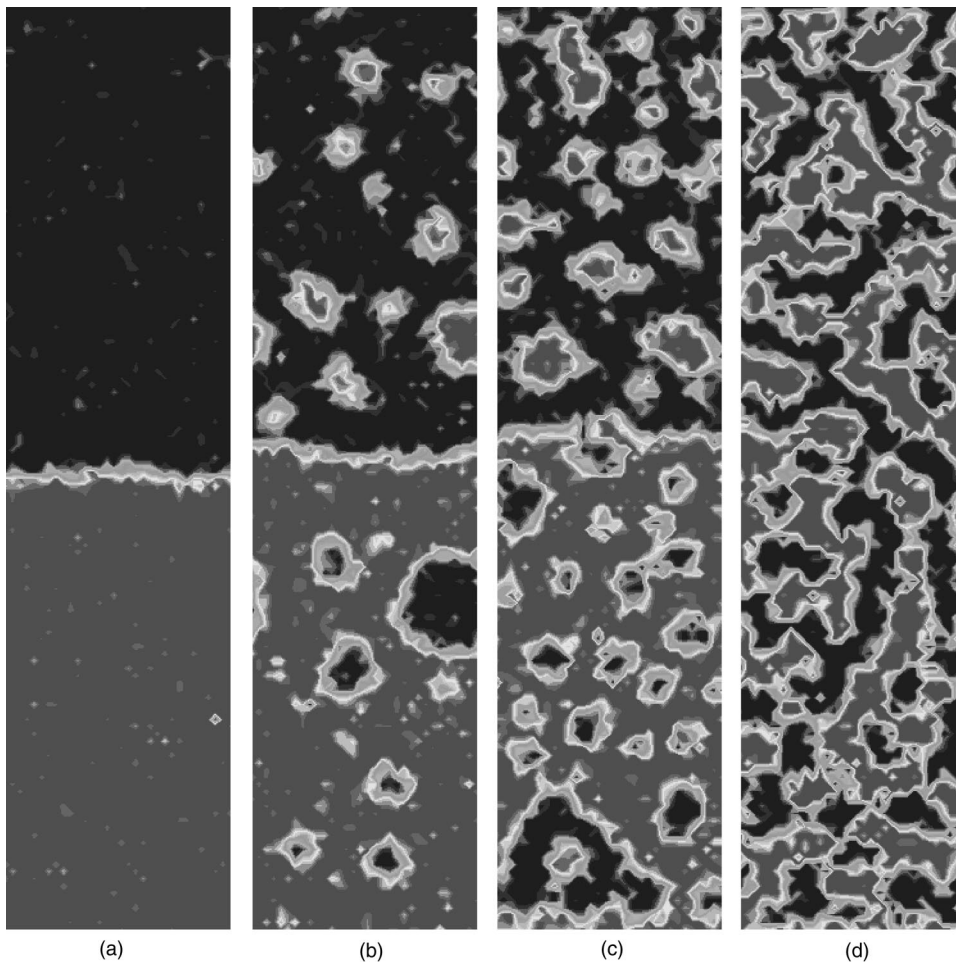


FIG. 10. Snapshots after 100 000 steps. Concentrations of added surfactant are (a) 0%, (b) 5%, (c) 25%, and (d) 50%. In case (d) the initial flat interface completely vanishes to form a bicontinuous phase. The measurement of the surface tension is meaningful as long as the initial flat interface is maintained, as shown in cases (a), (b), and (c). Color charges for hydrophilic and hydrophobic ends $C_{phi}=1.0$, $C_{pho}=-1.0$.

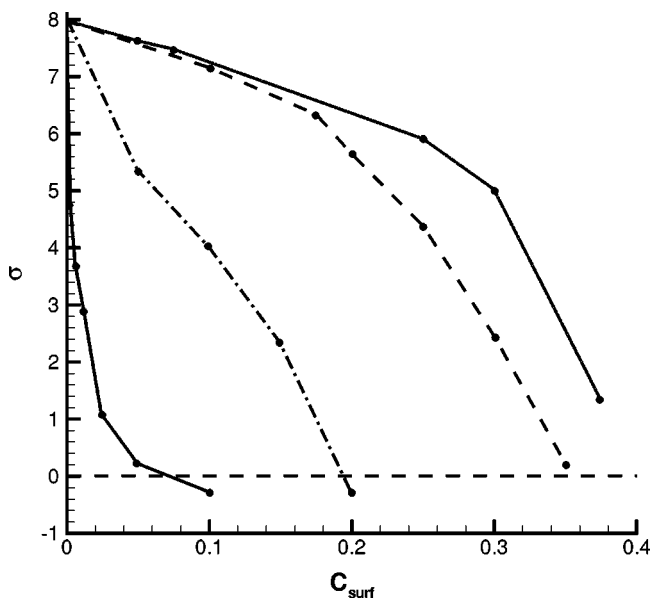


FIG. 11. The surface tension with varying amounts of surfactants in four sets of color charges for hydrophilic and hydrophobic ends C_{phi}, C_{pho} . From the rightmost, (C_{phi}, C_{pho}) are $(+1.0, -1.0)$, $(+2.5, -2.5)$, $(+5.0, -5.0)$, and $(+10.0, -10.0)$.

ered by the adsorption of the surfactant to interface, and the connection between the microscopic surfactant parameters and macroscopic surface tension behavior has been established.

It is worth mentioning that the model is simple enough to allow for a straightforward extension into 3D geometries. Three-dimensional version of this model has also been formulated and results will be published in the near future [13].

-
- [1] M. Laradji, O.G. Mouritsen, S. Toxvaerd, and J. Zuckermann, *Phys. Rev. E* **50**, 1243 (1994); L. Edwards and Y. Peng, in *Artificial Life VI*, edited by C. Adame *et al.* (MIT Press, Cambridge, 1998), pp. 35–42.
- [2] R.G. Larson, L.E. Scriven, and H.T. Davis, *J. Chem. Phys.* **83**, 2411 (1985); for recent reviews on Monte Carlo simulations of amphiphilic systems, see S. Bandyopadhyay, M. Tarek, and M.L. Klein, *Curr. Opin. Colloid Interface Sci.* **3**, 242 (1998).
- [3] A.N. Emerton, P.V. Coveney, and B.M. Boghosian, *Physica A* **239**, 373 (1997).
- [4] B.M. Boghosian, P.V. Coveney, P.J. Love, and J.-B. Malliet, *Mol. Simul.* **26**, 85 (2001); B.M. Boghosian, P.V. Coveney, and P.J. Love, *Proc. R. Soc. London, Ser. A* **456**, 1431 (2000).
- [5] J.-B. Malliet and P.V. Coveney, *Phys. Rev. E* **62**, 2898 (2000); P.J. Love, J.-B. Malliet, and P.V. Coveney (unpublished).
- [6] H. Chen, B.M. Boghosian, and P.V. Coveney, *Proc. R. Soc. London, Ser. A* **456**, 2043 (2000).
- [7] A. Malevanets and R. Kapral, *Europhys. Lett.* **44**, 552 (1998).
- [8] Y. Hashimoto, Y. Chen, and H. Ohashi, *Comput. Phys. Commun.* **129**, 56 (2000).
- [9] D.H. Rothman and J. Keller, *J. Stat. Phys.* **52**, 1119 (1988).
- [10] A review on such results can be found in W.R. Osborn, E. Orlandini, M.R. Swift, J.M. Yeomans, and J.R. Banavar, *Phys. Rev. Lett.* **75**, 4031 (1995).
- [11] A.N. Emerton, P.V. Coveney, and B.M. Boghosian, *Phys. Rev. E* **55**, 708 (1997).
- [12] T. Sakai, Y. Chen, and H. Ohashi, *Comput. Phys. Commun.* **129**, 75 (2000).
- [13] T. Sakai, Y. Chen, and H. Ohashi, *J. Colloid Surf.* (to be published).